A van der Waals density functional theory comparison of metal decorated graphene systems for hydrogen adsorption

Janet Wong, Shwetank Yadav, Jasmine Tam, and Chandra Veer Singh[a)]
Department of Materials Science and Engineering, University of Toronto, 184 College Street, Suite 140, Toronto, Ontario M5S 3E4, Canada

(Received 8 February 2014; accepted 28 May 2014; published online 9 June 2014)

Previous Density Functional Theory (DFT) studies on metal decorated graphene generally use local density approximation (LDA) or generalized gradient approximation (GGA) functionals which can cause inaccuracies in hydrogen binding energies as they neglect van der Waals (vdW) interactions and are difficult to compare due to their widely varying simulation parameters. We investigated the hydrogen binding ability of several metals with a consistent set of simulations using the GGA functional and incorporated vdW forces through the vdW-DF2 functional. Metal adatom anchoring on graphene and hydrogen adsorption ability for both single and double sided decoration were studied for eight metals (Al, Li, Na, Ca, Cu, Ni, Pd, and Pt). It was found that the vdW correction can have a significant impact on both metal and hydrogen binding energies. The vdW-DF2 functional led to stronger metal adatom and hydrogen binding for light metals in comparison to GGA results, while heavier transition metals displayed the opposite behaviour but still produced stronger hydrogen binding energies than light metals. Nickel was found to be the best balance between hydrogen binding ability for reversible storage and low weight. The effects on hydrogen binding energy and maximum achievable hydrogen gravimetric density were analyzed for Ni-graphene systems with varying metal coverage. Lower metal coverage was found to improve hydrogen binding but decrease hydrogen gravimetric density. The highest achieved Ni-graphene system gravimetric density was 6.12 wt. %. © *2014 AIP Publishing LLC*.
[http://dx.doi.org/10.1063/1.4882197]

I. INTRODUCTION

In the past few years, there has been an increasing interest in using solar hydrogen as a clean alternative fuel.[1] Presently, one of the main issues associated with hydrogen fuel technology is its energy storage capacity, which is still far from being able to compete with fossil fuels.[2,3] For hydrogen storage systems in transportation applications, the U.S. Department of Energy (DOE) has set a target of achieving a hydrogen gravimetric capacity of 5.5 wt. % and a volumetric capacity of 0.04 kg/m^3 by 2015.[4] One approach for room temperature storage is through the adsorption of hydrogen on substrate materials. Among proposed substrates, including hydrides, zeolites, and metal organic frameworks, porous carbon structures are some of the most appealing.[5] These substrates are low in weight and have the potential to be the most economically viable. Within this class of materials is graphene, a single layer of carbon atoms with a unique 2D structure which gives it a large specific surface area and great mechanical strength. These properties make graphene an ideal material for hydrogen adsorption.[2]

Molecular hydrogen, as found in its gaseous form for practical storage devices, adhers to graphene through physisorption. However, for the case of pristine graphene, this process is too weak for it to stably bind enough hydrogen molecules to reach the DOE hydrogen density targets.[6] Metal decoration of graphene sheets shows potential in increasing their hydrogen adsorption ability to levels required for the DOE targets.[7,8] In such cases, the hydrogen molecules generally bind to the metal atoms through physisorption, although they may dissociate and chemisorb due to the influence of some metals.[6] Theoretical studies conducted on metal decorated graphene systems predict very high gravimetric densities which easily surpass the DOE target. For instance, it has been claimed that a Li decorated system can achieve 16 wt. % hydrogen storage,[8] Al decoration can achieve 13.8 wt. %,[9] and Ca decoration can achieve 8.4 wt. %.[10] Contrary to these theoretical studies, the experimental results for metal decorated graphene have fallen far short of these numbers and none have been able to achieve greater than 2 wt. % at room temperature.[11–14] Theoretical predictions are generally made with density functional theory (DFT) calculations using local density approximation (LDA) and generalized gradient approximation (GGA) functionals. It should be noted that this can cause inaccuracies associated with hydrogen binding energy values as generally they can be overestimated by LDA or underestimated by GGA. The LDA functional is usually inaccurate for interactions in such complex systems, while the GGA functional is accurate for strong covalent type forces but neglects van der Waals (vdW) interactions. For metal decorated graphene systems, vdW interactions are significant for describing the physisorption of hydrogen and the interaction between neighboring metal atoms, especially at higher coverages[7,8] and this might be one reason as to why experimental results fall short of theoretical assertions. A recent study which attempted to

[a)]Electronic mail: chandraveer.singh@utoronto.ca

consider the effect of vdW forces in Ca decorated graphene[7] hints at this as it concluded that the system could only achieve a gravimetric density of 2.6 wt. %, a marked decrease from previous claims. Amongst theoretical studies, the highest gravimetric densities have been generally achieved for light metals. However, it is difficult to compare different metal predictions as various studies use widely varying exchange-correlation functionals, pseudopotentials, and simulation parameters. Therefore, a comprehensive understanding of the realistic hydrogen binding ability of metal decorated systems is currently lacking.

This study compares the hydrogen binding ability of several metal adatoms on graphene and evaluates the importance of including vdW interactions, incorporated using the vdW-DF2 functional. This should help provide a more accurate prediction for the hydrogen binding ability of each atom in comparison to earlier studies. In total, four light metals and four transition metals were investigated. Nickel was determined to be the best overall metal system for reversible storage and likely to produce the highest gravimetric density. Using nickel-graphene systems, changes in binding abilities were investigated for varying metal decoration coverage. The gravimetric density for these varying metal coverage nickel-graphene systems was also investigated by adsorbing multiple hydrogen molecules.

II. COMPUTATIONAL DETAILS

The hydrogen storage capacity of a metal decorated graphene sheet was studied using first principles methods based on DFT. The DFT calculations were performed with Quantum-Espresso[15] which uses the plane-wave pseudopotential approach. The GGA functional described by Perdew-Burke-Ernzerhof (PBE)[16] was used to describe the exchange-correlation of electrons. Ultrasoft pseudopotentials were used for all calculations.[17] Van der Waals interactions were modeled by adding a correction to the GGA functional, when applied, through the vdW-DF2 functional.[18] This functional was used instead of the earlier vdW-DF[19] for increased accuracy in estimating the equilibrium separation, H_2 bond strengths, and van der Waals attractions at intermediate separation longer than equilibrium ones.[18] The kinetic energy cutoff value was set to 60 Ry for the wave functions and to 600 Ry for the charge density. The supercell and atomic positions were optimized using the conjugate gradient algorithm. The convergence threshold was set to 7E-7 Ry for self consistency in energy and to 8E-3 a.u. for forces. The total energy convergence was maintained at $\leq$5 meV/atom.

The metal-graphene systems for comparing different metals were modeled with 1×1 supercells (6 C atoms) and a vacuum layer thickness $\geq$20 Å. The Brillouin zone was sampled using a $8 \times 8 \times 1$ Monkhorst-Pack[20] k-point grid and Methfessel-Paxton[21] smearing of 0.01 Ry.[22] In addition, each metal adatom was placed at its most stable adsorption site on the graphene sheet according to literature. Based on previous work by Wang *et al.*[7] and Sigal *et al.*,[23,24] the most favorable adsorption site for Al, Ca, Li, Na, and Ni on graphene is at the "hollow" position, while Pd and Pt prefer the "bridge" position and Cu prefers the "top" position.

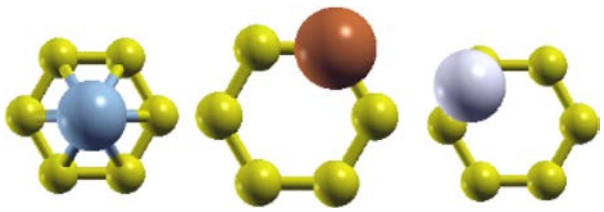

FIG. 1. Possible adsorption sites for metal atoms. From left to right, the adatom is at the hollow site, the top site and the bridge site, respectively.

See Figure 1 for the schematic diagram of the different binding sites. Simulations investigating metal coverage and gravimetric density were conducted with a single metal adatom placed on each side of the graphene sheet (to give a total of two metal adatoms in the entire supercell) and varying the number of surrounding carbon atoms.

The binding energy of a metal atom on graphene was calculated as

$$E_b = -[E_{graphene+nmetal} - (E_{graphene} + nE_{metal})]/n, \quad (1)$$

where $E_{graphene+nmetal}$ is the total energy of the graphene sheet with either single- or double-sided metal decoration, $E_{graphene}$ is the total energy of the pristine graphene sheet, E_{metal} is the total energy of the free metal adatom, and n corresponds to the number of metal adatoms.

The average binding energy per hydrogen molecule was calculated with the following equation:

$$E_b = -[E_{metal-graphene+iH_2} - (E_{metal-graphene} + iE_{H_2})]/i, \quad (2)$$

where $E_{metal-graphene+iH_2}$ is the total energy of the hydrogen adsorbed on the metal-graphene system, $E_{metal-graphene}$ is the total energy of the metal-graphene sheet, E_{H_2} is the total energy of the free H_2 molecule, and i corresponds to the number of H_2 molecules. All atomic and charge density visualizations were created using XCrySDen[25] and VESTA.[26]

III. RESULTS AND DISCUSSION

In this section, we first report the adsorption energy of metal adatoms over graphene sheets for eight metals and consider both single and double sided metal decoration. Thereafter, adsorption of hydrogen molecules over different metal-decorated systems is described, considering the same substrate size among the investigated metals. A careful analysis of these hydrogen adsorption studies pointed to Ni as the most promising metal adatom. Thus, a more thorough investigation was conducted for the Ni decorated graphene system to understand the effect of substrate size, and determine its optimum hydrogen adsorption capability.

The effect of spin polarization was determined by comparing the binding energies of metal decorations on graphene using only GGA with and without spin polarization. Spin polarization has not yet been implemented for the vdW-DF method in Quantum Espresso. Therefore, all simulations with the vdW-DF2 functional were performed without spin polarization. For the GGA simulations, it was determined that spin polarization had no significant effect on the metal binding energy of any of the metals. For hydrogen

TABLE I. Binding energies (eV), vertical adatom distance with respect to graphene sheet (Å), and literature values (Lit.) for single sided metal decoration. The adatom positions over graphene are indicated in brackets, where H stands for adatom at the hollow, B stands for adatom on the bridge between two carbon atoms, and T stands for adatom above a carbon atom.

	E_b (eV)			$d_\perp$ (Å)			
System	GGA	vdW-DF2	Lit.	GGA	vdW-DF2	Lit.	Literature notes
AlC_6 (H)	0.03	0.22	0.82	2.06	3.49	2.08	System was C_8 with 18 Å c-axis using LDA PP[9]
LiC_6 (H)	−0.43	0.17	1.00	5.99	1.91	1.88	System was C_6 with 16 Å c-axis using GGA-PBE and PAW PP[8]
NaC_6 (H)	−0.01	0.04	0.59	2.70	2.81	…	System was C_{60} with 20 Å c-axis using GGA-PBE, localized basis sets and norm-conserving PP[23]
CaC_6 (H)	0.52	0.50	2.19, 1.53, 1.60	2.33	2.49	…	(LDA, GGA, and vdW-DF, respectively) System was C_6 with 20 Å c-axis with indicated functionals[7]
CuC_6 (T)	0.15	0.17	0.39	2.14	3.21	…	System was C_{60} with 20 Å c-axis using GGA-PBE, localized basis sets and norm-conserving PP[23]
NiC_6 (H)	1.27	0.48	1.99	1.59	1.77	1.65	System was C_{24} with 20 Å c-axis using GGA-PBE, localized basis sets and norm-conserving PP[24]
PdC_6 (B)	0.76	0.48	1.08	2.12	2.34	2.25	System was C_{24} with 20 Å c-axis using GGA-PBE, localized basis sets and norm-conserving PP[27]
PtC_6 (B)	1.13	0.66	1.73	2.03	2.15	…	System was C_{60} with 20 Å c-axis using GGA-PBE, localized basis sets and norm-conserving PP[23]

adsorption, only Ni, Pd, and Pt demonstrated a small sensitivity to spin polarization. Therefore, these three metal systems had both spin and no-spin calculations conducted while studying hydrogen adsorption with the GGA functional alone. There was a less than 0.01 eV difference due to spin polarization for Ni and Pd and less than 0.6 eV difference for Pt in these results.

A. Metal anchoring over graphene

The overall stability of each metal-graphene system, prior to hydrogen adsorption, was analyzed by calculating the binding energy of the metal adatom on graphene for both the single- and double-sided decoration cases. According to Eq. (2), a positive binding energy indicates that the metal adatom is stably bound to graphene in its ground state. The binding ability results for the single- and double-sided metal decoration are listed in Tables I and II, respectively, along with the equilibrium distances of each adatom from the graphene sheet. In both cases, the vdW-DF2 results show that all metal atoms bind to graphene, while all metals with the exception of Li and Na do so for the GGA simulations. The transition metals generally show stronger binding than light metals with the exception of Ca, which has quite strong binding, and Cu, which has relatively weak binding. The metals with strong binding metals all have unfilled d-shells (including the non-transition Ca), suggesting that this may be a possible cause for a stronger bond as their less stable nature may cause them to be more likely to share charge with the graphene electrons. This would also explain the lower binding energy for Cu, despite it being a transition metal, as it has a filled d-shell. Figure 2 points to another difference between the graphene anchored light and transition metals by comparing the charge densities of Al and Ni. Both the charge density difference for metal adatom adsorption and charge density isosurface at a value of 0.14 (number of charge/Bohr^{-3}) are shown for each metal type. The figure indicates that there is a greater charge loss from around the Al atoms (Fig. 2(b)), especially at the ends facing away from the graphene sheet which are most likely to interact with hydrogen molecules, than from around

TABLE II. Binding energies per atom (eV), vertical adatom distance with respect to graphene sheet (Å), and literature values (Lit.) for double sided metal decoration. The adatom positions over graphene are indicated in brackets, where H stands for adatom at the hollow, B stands for adatom on the bridge between two carbon atoms, and T stands for adatom above a carbon atom.

	E_b (eV)			$d_\perp$ (Å)			
System	GGA	vdW-DF2	Lit.	GGA	vdW-DF2	Lit.	Literature notes
Al_2C_6 (H)	0.15	0.21	0.96	2.26	3.55	2.14	System was C_8 with 18 Å c-axis using LDA PP[9]
Li_2C_6 (H)	−0.37	0.18	0.99	6.05	1.86	1.85	System was C_6 with 16 Å c-axis using PBE-GGA and PAW PP[8]
Na_2C_6 (H)	−0.01	0.03	…	2.08	2.16	…	…
Ca_2C_6 (H)	0.66	0.64	2.33, 1.63, 1.69	2.31	2.39		(LDA, GGA, and vdW-DF, respectively) System was C_6 with 20 Å c-axis with indicated functionals[7]
Cu_2C_6 (T)	0.14	0.18	…	2.26	3.35	…	…
Ni_2C_6 (H)	1.18	0.49	…	1.63	1.83	…	…
Pd_2C_6 (B)	0.64	0.43	…	2.18	2.46	…	…
Pt_2C_6 (B)	0.84	1.00	…	2.16	2.17	…	…

the Ni atoms (Fig. 2(a)). Furthermore, the Ni atoms have greater charge density around them, whereas the Al atoms show no noticeable charge surrounding them. This indicates that the Ni atom will have more charge available for interaction with hydrogen atoms.

There are four additional trends observed from both Tables I and II. First, going from single- to double-sided decoration generally increased the binding energy of each metal adatom. The exceptions, Na and Pd, showed insignificant decreases of less than 0.1 eV which can be ignored when considering the advantages gained by having the ability to bind hydrogen on both sides of the graphene sheet. Hence, double sided decoration is preferred for hydrogen adsorption. Second, for single sided decoration, light metals (Al, Li, Na, and Ca) generally show an increased binding energy with vdW-DF2 functional as compared to GGA only simulations, while transition metals depict the opposite trend. For double sided decoration, this trend holds except for Ca and Pt, perhaps reflecting the particular nature of each metal and the manner in which its valence shells interact. The tables also present literature values for the metal binding energies. Our GGA and vdW-DF2 metal binding values are consistently lower than both LDA and GGA results found in literature. The higher literature LDA values are expected as the functional is known to overestimate binding. The reasons for the difference between our GGA results and those from literature are likely due to very different metal coverage and simulation parameters such as vacuum spacing, pseudopotential, and software implementation, partially described in the "Literature notes" section of Tables I and II. We have tried to produce highly accurate GGA simulations by using vacuum spacing much larger than previous studies as we found interlayer interactions even at the spacing level of the previous studies, as well as stringent energy cutoffs and a high number of k-points. As a third trend, there is a distinct pattern observed for transition metal vdW-DF2 results that is less apparent in the calculations made using only GGA. The binding energy tends to increase as the number of d-electrons increases. However, when the number of d-electrons increases to more than half occupancy, the binding energy starts to decrease. Finally, the distance of the adatom from the graphene sheet is greater for vdW-DF2 results than GGA only results for all cases. This trend may be due to the presence of stronger long range interactions allowed in vdW-DF2, which allows the metal atom to be energetically stable at a farther distance from the graphene sheet. On the other hand, GGA simulations without vdW corrections would require greater proximity to feel the same level of attractive force. It should be pointed out that while the earlier vdW-DF functional tended to overestimate distances, the vdW-DF2 functional has improved distance estimation[18] and hence we expect the present results to be more accurate.

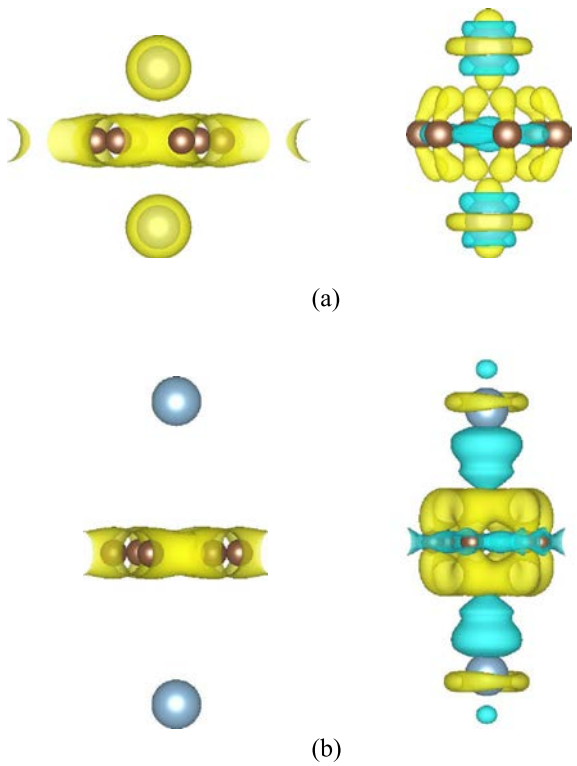

FIG. 2. Isosurfaces of charge density and charge density difference for (a) Ni and (b) Al adatoms adsorbed on graphene. In the charge density difference isosurfaces, yellow indicates regions of charge gain and blue indicates regions of charge loss. The Al atoms, a light metal, show greater charge loss and a smaller region of remaining charge density than the heavy metal Ni atoms. This might be one reason for heavier metal atoms possessing stronger hydrogen binding energy as they have greater charge which can interact with hydrogen molecules.

B. Hydrogen adsorption on metal-decorated graphene

The binding energy for the adsorption of a single hydrogen molecule on each metal adatom is summarized in Table III. Since previous calculations showed that double-sided metal decoration is more stable in most cases, the hydrogen adsorption energies were calculated for that configuration only. GGA calculations with and without spin polarization are also included for the transitions metals Ni, Pd, and Pt. These GGA results confirmed that spin polarization can be ignored for Ni and Pd, while Pt does show a difference of 0.6 eV in binding energy owing to its inclusion. However, this difference in energy for Pt is not large enough to affect its comparison to other metals and our conclusions from the simulations remain unaffected. As stated earlier, the vdW-DF2 functional has not been be implemented with spin-polarization in Quantum Espresso at present and so only unpolarized simulations were conducted for this functional. For the light non-transition metal adatoms (Al, Ca, Na, Li), the vdW-DF2 results produced higher binding energies than GGA results by an order of magnitude but were still much weaker than those of the transition metals. For the heavier transition metals, the GGA results produced stronger binding energies than vdW-DF2 results; although the difference was not an order of magnitude. The difference occurring due to the vdW-DF2 correction can be analyzed by looking at the partial density of states (PDOS) of the Ni system, as shown in Figure 3. The PDOS for the GGA simulation shows a greater number of peaks and wider distribution for the Ni d-shell compared to the plotted PDOS after including the vdW-DF2 functional. This indicates that the GGA Ni has more localized distinct energy states which are likely to

TABLE III. Average hydrogen binding energy (eV/H_2) for metal graphene system. The adatom positions over graphene are indicated in brackets, where H stands for adatom at the hollow, B stands for adatom on the bridge between two carbon atoms, and T stands for adatom above a carbon atom.

	E_b (eV)				
System	GGA (no-spin)	GGA (spin)	vdw-DF2 (no-spin)	Literature value	Literature notes
Al_2C_6-$2H_2$ (H)	0.004	…	0.044	$E_b = 0.2$ eV (Ref. 9)	System was C_8 with 18 Å c-axis using LDA PP
Li_2C_6-$2H_2$ (H)	0.356	…	0.118	$E_b = 0.10$ eV (Ref. 8)	System was C_6 with 16 Å c-axis using GGA-PBE and PAW PP
Na_2C_6-$2H_2$ (H)	0.021	…	0.000	$E_b = 0.02$ eV (Ref. 23)	System was single-side decorated C_{60} with 20 Å c-axis using GGA-PBE, localized basis sets and norm-conserving PP
Ca_2C_6-$2H_2$ (H)	0.007	…	0.025	$E_b = 0.03$ eV (LDA), 0.01 eV (GGA), 0.06 eV (vdW-DF) (Ref. 7)	System was C_6 with 20 Å c-axis with indicated functionals
Cu_2C_6-$2H_2$ (T)	0.506	…	0.262	$E_b = 0.04$ eV (Ref. 23)	System was single-side decorated C_{60} with 20 Å c-axis using GGA-PBE, localized basis sets and norm-conserving PP
Ni_2C_6-$2H_2$ (H)	0.268	0.267	0.171	$E_b = 1.21$ eV (Ref. 24)	System was single-side decorated C_{24} with 20 Å c-axis using GGA-PBE, localized basis sets and norm-conserving PP
Pd_2C_6-$2H_2$ (B)	0.843	0.842	0.510	$E_b = 1.86$ eV (Ref. 27)	System was single-sided C_{24} with 20 Å c-axis using GGA-PBE, Localized basis sets and norm-conserving PP
Pt_2C_6-$2H_2$ (B)	1.75	1.15	1.02	$E_b = 1.65$ eV (Ref. 23)	System was single-side decorated C_{60} with 20 Å c-axis using GGA-PBE, localized basis sets and norm-conserving PP

more strongly interact and share charge with hydrogen molecules. On the other hand, the reduced number of peaks in the vdW-DF2 Ni indicates that its d-shell is filled due to greater charge sharing with the graphene substrate. It is thus more stable and less likely to strongly interact with a hydrogen molecule. Consequently, the vdW-DF2 simulated Ni will have a weaker hydrogen binding energy than the GGA simulated Ni. The increased sharing of charge between the Ni atoms and the graphene substrate when vdW corrections are included also helps to explain why the vdW-DF2 simulation showcased a stronger metal binding energy than the GGA simulation. These results reinforce that vdW interactions can affect the charge distribution in a metal decorated system and its hydrogen binding ability and should be taken into account when modelling such systems. Amongst the considered metals, Pt possessed the strongest hydrogen binding ability, while Na possessed the weakest.

After system relaxation, both the GGA and vdW-DF2 simulations displayed the formation of a complex involving a hydrogen molecule and metal adatoms for the transition metals (Cu, Ni, Pd, and Pt), as can be seen from Figure 4. This complex, involving the dissociation of the H-H bond, corresponds to structure III described previously by Lopez-Corral[27] for their H_2-Pd-graphene system. The H-H distance after adsorption for our Pd-graphene system was about 0.80 Å. The H-H distance after adsorption for Lopez-Corral's Pd-graphene system with single-sided metal decoration ranges from 0.85 to 0.87 Å. The formation of the complex is likely the cause for the much stronger binding energies of the transition metals as the hydrogen atoms move towards a more chemical type of adsorption.

Optimal binding energies for reversible hydrogen storage should lie within the range of 0.2–0.6 eV per H_2 molecule.[9] If the binding energy is too high, then releasing the hydrogen molecules will be difficult at moderate operating conditions. If the converse occurs then the storage of hydrogen will be minimal. Based on our results, three metal-graphene systems fulfill this optimal criterion. The Cu-graphene system displayed a hydrogen binding energy of 0.51 eV for GGA only results and 0.26 eV for vdW-DF2 results. The Ni-graphene system had a hydrogen binding energy of 0.27 eV for GGA only results and 0.17 eV for vdW-DF2 results. Lastly, the Pd-graphene system demonstrated a hydrogen binding energy of 0.84 eV for GGA only results and 0.51 eV for vdW-DF2 results. The GGA binding energy value for Pd is too high and outside of the optimal range of values 0.2–0.6 eV, while the vdW-DF2 value for Ni is just lower than the lower limit of preferred values. The vdW-DF2 result of Ni is outside of the needed range of values by only 0.03 eV, which is a small enough difference to effectively still consider Ni suitable for reversible storage. The slight improvement needed in binding ability may be provided by moderately increased gas pressure or other techniques.

As the goal of the studied metal-graphene systems is to maximize hydrogen gravimetric density, a heavy metal mass is disadvantageous as it would reduce the relative mass percentage of hydrogen in the system. Among the three selected metals best suited for reversible hydrogen storage, the increased binding energies of Pd and Cu compared to Ni will allow them to bind more hydrogen molecules. However, Pd and Cu are also heavier than Ni and this offsets any advantage offered by the few additional hydrogen molecules they can adsorb. Hence, binding more hydrogen molecules "does" not necessarily lead to higher hydrogen mass percentage in the system. Nickel provides the best balance by still having a fairly strong hydrogen binding ability, while possessing the lowest mass of the studied transition metals. The nickel-graphene system also showed the strongest binding to the

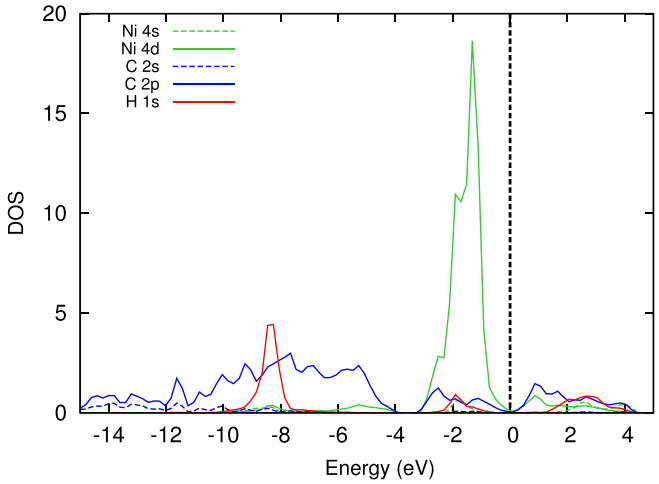

(a)

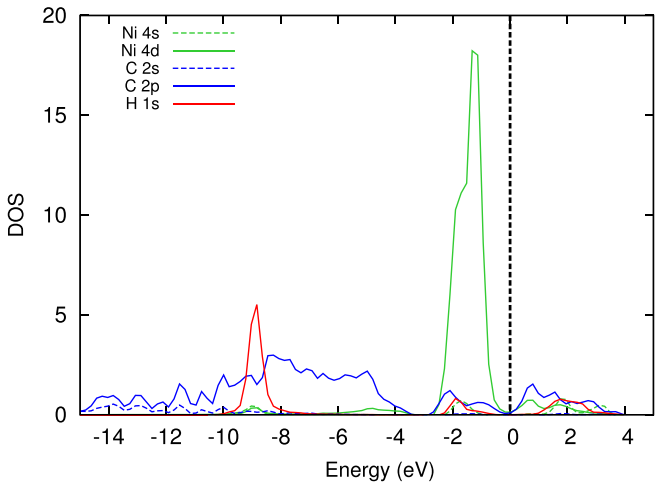

(b)

FIG. 3. PDOS of Ni-graphene system simulations with (a) GGA functional alone and (b) GGA functional with vdW-DF2 corrections. The greater number of peaks and width of the Ni d-shell orbital for (a) indicates more distinct localized energy states and stronger potential for interaction with a hydrogen molecule.

graphene substrate among the three selected candidates, making it the most stable among the three. Furthermore, investigations conducted by Sigal *et al.*[24] observed that chemical treatment can be used to deposit nickel compounds onto a graphene surface, suggesting experimental feasibility of a nickel-graphene system. In the same study, nickel was determined to be less easily oxidized than other metal decorations. Oxidation may occur in real world situations where

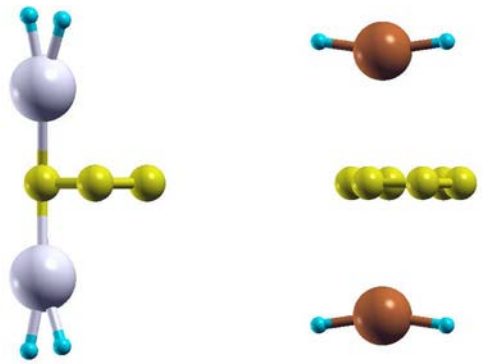

FIG. 4. Examples of the hydrogen-metal complexes formed by transition metals, palladium on the left and copper on the right. The hydrogen molecule has dissociated and moved towards a chemisorbed state, producing stronger hydrogen binding energies for transition metals.

the system is exposed to air and acts as a strong inhibitor for hydrogen adsorption. The combination of strong hydrogen binding ability suited to reversible storage, relatively low mass and increased practical feasibility due its highly stable metal-graphene system and resistance to oxidation make nickel the best candidate for use in a metal decorated graphene hydrogen storage system. Therefore, nickel was selected for use in all subsequent simulations looking at metal coverage and maximum gravimetric density.

C. Optimal hydrogen storage on Ni-decorated graphene

1. Effect of varying Ni coverage

The effect of metal coverage, described by the relative density of or equivalently the distance between metal adatoms on the graphene sheet, can be quite significant due to the complex mix of attractive and repulsive forces acting within each system. As observed by Wang *et al.*,[7] changes in metal adatom distance result in variations in interaction energy between adatoms, thus influencing their binding abilities with the hydrogen molecules. Since each simulation uses a repeating supercell with a single metal adatom on each side of the graphene sheet, the size of the graphene substrate supercell determines the metal coverage of the system. The small 6 carbon supercell used for the simulations comparing different metal systems represents the highest metal coverage where metal adatoms have the shortest distance between them. Four supercells of increasing size (6, 16, 32, and 72 carbon atoms as seen in Figure 5) were simulated

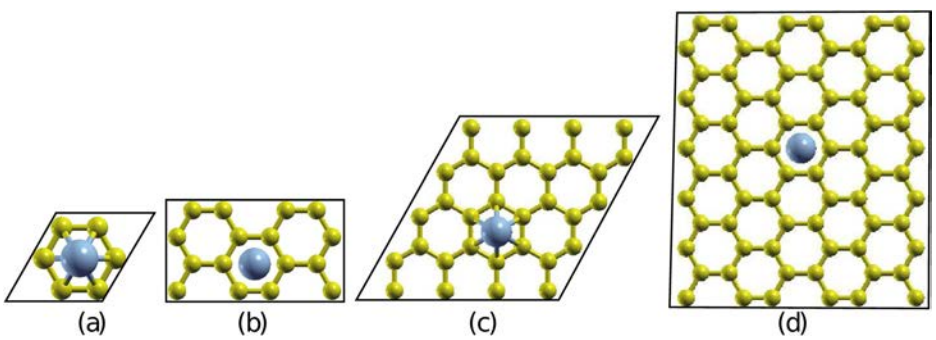

FIG. 5. Supercells used for differing Ni metal coverage simulations: (a) 6 carbon atoms, (b) 16 carbon atoms, (c) 32 carbon atoms, and (d) 72 carbon atoms.

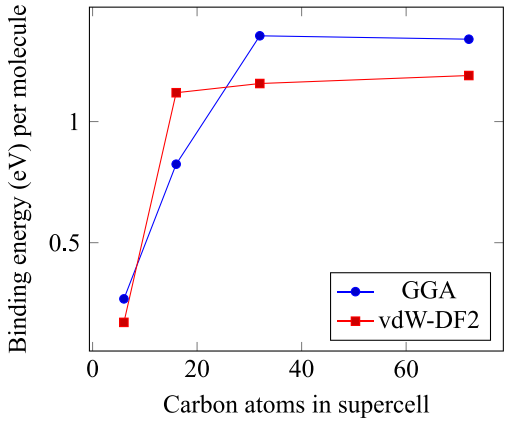

FIG. 6. Average hydrogen binding energy (eV/H_2) for Ni-decorated graphene systems at different substrate sizes.

with GGA alone and with vdW-DF2 included. The results are presented in Figure 6.

In general, an increase in supercell size yielded an increase in hydrogen adsorption binding energy. The 32 carbon atom graphene substrates provided the highest binding energy for GGA only results (just slightly higher than 72 atoms), while the 72 carbon atom supercell provided the highest energy for vdW-DF2 results. This suggests that at close range, the proximity of metal atoms has a negative effect on hydrogen binding ability. This might be due to the increased stability felt by the closer metal atoms, making the hydrogen molecule less attractive to them for achieving stability. There might also be repulsive forces between hydrogen molecules at such close range, as they become partially charged after donating electronic charge towards the metal adatoms. The finding that increased supercell size leads to higher binding energy suggests that lower metal coverage might be beneficial for hydrogen storage. However, an increased supercell size also increases the number of carbon atoms and this will very quickly outweigh any gains from additional adsorbed hydrogen. Hence, a balance must be found between the need for fewer carbon atoms per metal adatom to decrease non-hydrogen mass and for larger supercells to increase hydrogen binding energies. It should be noted that the lower metal cover simulations all produce strong hydrogen binding energies outside the range of −0.2 to −0.6 eV preferred for reversible storage.

TABLE IV. Average hydrogen binding energy (eV/H_2) for increasing number of adsorbed hydrogen molecules and different substrate sizes (in terms of number of carbon atoms). Dashed lines indicate a simulation was not conducted, due to low chance of adsorption for 6 C or low gravimetric density for 32 C. The 16 C substrate represents the best balance of substrate size and binding energy which allows it to meet the DOE's goal of 5.5% gravimetric density.

	Number of hydrogen molecules				
Graphene substrate	2	4	6	8	10
6 C	0.171	−2.148	Not converged	−0.956	…
16 C	1.119	0.470	0.323	0.260	0.232
32 C	1.157	0.638	0.160	0.261	…

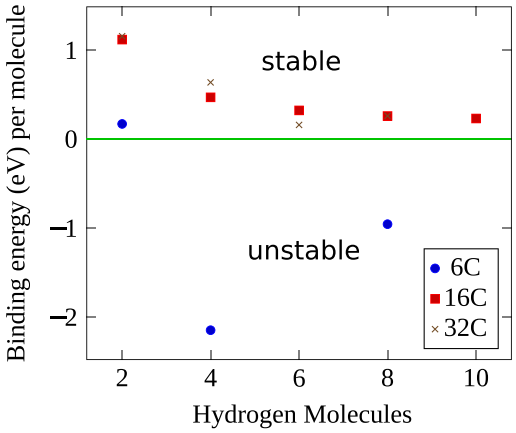

FIG. 7. Average hydrogen binding energy (eV/H_2) for increasing number of adsorbed hydrogen molecules and different substrate sizes (in terms of number of carbon atoms).

2. Maximum gravimetric density for Ni graphene systems

The gravimetric density for each varying metal coverage system studied in Subsection III C 1 was investigated by adding increasing numbers of hydrogen molecules to each metal adatom. The results of the gravimetric density simulations and average hydrogen molecule binding energy are presented in Table IV and Figure 7, while Figure 8 presents the theoretical gravimetric density numbers for each system if the hydrogen molecules successfully adsorbed. The 6 carbon atom supercell fails to bind more than two hydrogen molecules, with higher numbers of molecules producing negative binding energies or failing to converge in their simulations which would suggest unstable configurations. This is caused by the relatively lower binding energy for this metal coverage as discussed in Subsection III C 1, which prevents the binding of large numbers of hydrogen molecules and hence simulations were stopped after attempting to adsorb 8 molecules. Note that the 6 carbon substrate also has the highest theoretical gravimetric density for each number of hydrogen molecules, indicating it is preferable to have higher metal adatom coverage. The 16 carbon atom supercell is the next

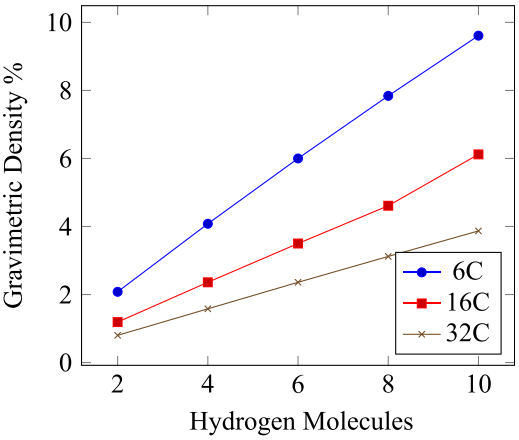

FIG. 8. Maximum theoretical hydrogen gravimetric density (wt. %) for different number of adsorbed hydrogen molecules and substrate sizes (in terms of number of carbon atoms). Note that not all of the systems successfully adsorbed the hydrogen molecules (see Figure 7).

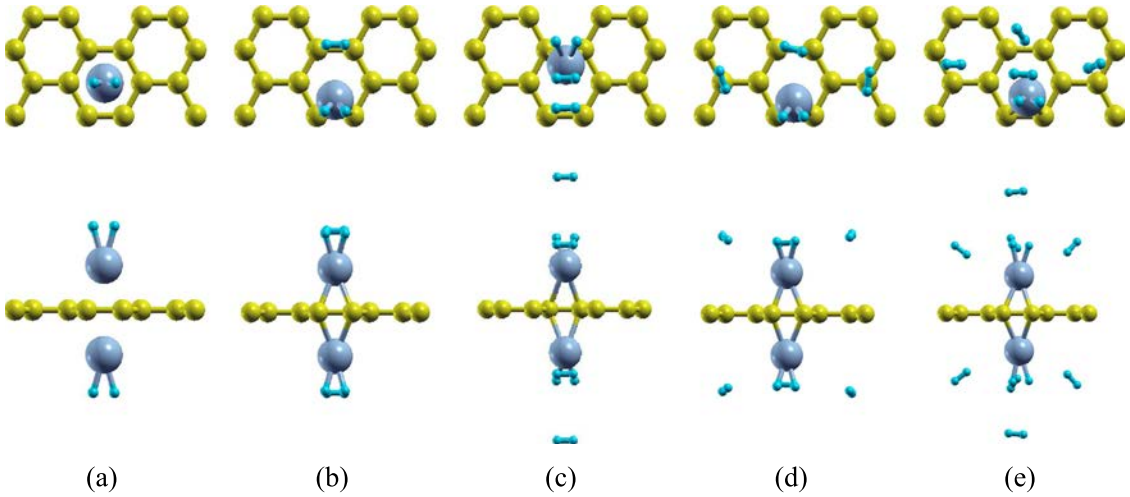

FIG. 9. Configurations of adsorbed hydrogen on the 16 carbon Ni decorated supercell, with increasing numbers of hydrogen molecules: (a) 2, (b) 4, (c) 6, (d) 8, and (e) 10.

smallest substrate and has a high enough binding "ability" to adsorb up to 10 hydrogen molecules. This is also the point at which this substrate is able to surpass the DOE goal of 5.5% gravimetric density, achieving 6.2 wt. %. Hence, the 16 carbon substrate is able to provide a good balance between having a supercell size which allows high gravimetric densities and binding energies strong enough to adsorb multiple hydrogen molecules. The configurations for the increasing numbers of hydrogen molecules can be seen in Figure 9. A correlation between the gravimetric density and average binding energy for the 16 carbon substrate is shown in Figure 10, where a rapid drop of binding strength with increasing number of hydrogen molecules shows the importance of vdW interactions as the binding strength moves away from the chemisorption type of binding towards weaker physisorption strengths. The final data point for the maximum 10 hydrogen molecules is just within the desired range of −0.2 to −0.6 eV. The PDOS of the 16 carbon substrate with the different number of hydrogen molecules adsorbed are shown in Figure 11. The distance of the hydrogen from the Fermi level and the lack of overlap between

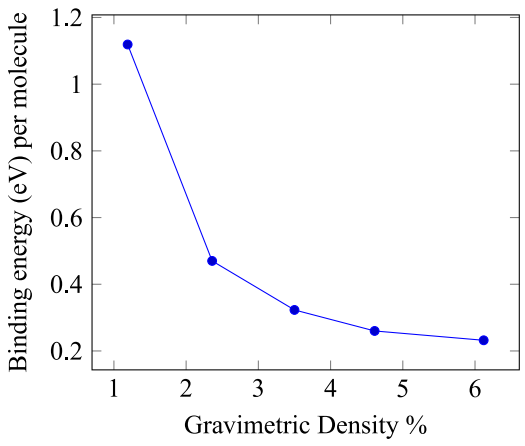

FIG. 10. Correlation between hydrogen gravimetric density (wt. %) and average binding energy (eV/H_2) for the 16 carbon substrates.

hydrogen and Ni peaks indicates that the hydrogen is not binding through a Kubas type interaction,[28] despite the fact that Ni has unfilled d-shells. This would then suggest that the hydrogen binds by a weak electrostatic dipole mechanism. This is further confirmed by looking at the charge density difference for two adsorbed hydrogen molecules in Figure 11(f), where sharp charge accumulation and depletion zones around the hydrogen atoms indicate polarization of the hydrogen molecule. As expected, the number of states for hydrogen increase as the number of adsorbed hydrogen molecules increase. Another interesting aspect is the interaction between hydrogen molecules which is visible as the peaks of hydrogen change in number and spread with different numbers of molecules. The system with 6 hydrogen molecules has the most distinct peaks, demonstrating a broad range of occupancies for quite differently configured hydrogen molecules. For the 10 molecules system, the number of peaks goes down again to two while the number of states at these two peaks' energies increases, indicating overlap and stabilization in the more symmetrically configured molecules.

The 32 carbon atom substrate initially showed the highest binding energy as expected but surprisingly produced lower average binding energies than the 16 carbon substrate for increasing numbers of hydrogen molecules. This might be because the increased distance between hydrogen molecules adsorbed to different metal adatoms allows them to interact and stabilize each other to a lower extent, whereas this distance seems to be closer to optimal for the 16 carbon substrate and too small for the 6 carbon substrate. The 32 carbon substrate also has very low theoretical gravimetric densities and hence no simulations were attempted beyond 8 hydrogen molecules as they would not be able to meet the DOE's target. By the same reasoning, the 72 carbon atom supercell would have had particularly low gravimetric densities due to the large number of carbon atoms and was thus excluded from the gravimetric density simulations altogether. This addresses the point discussed in Subsection III C 1, where the increased binding energy of larger supercells comes at the price of more carbon atoms which negate any

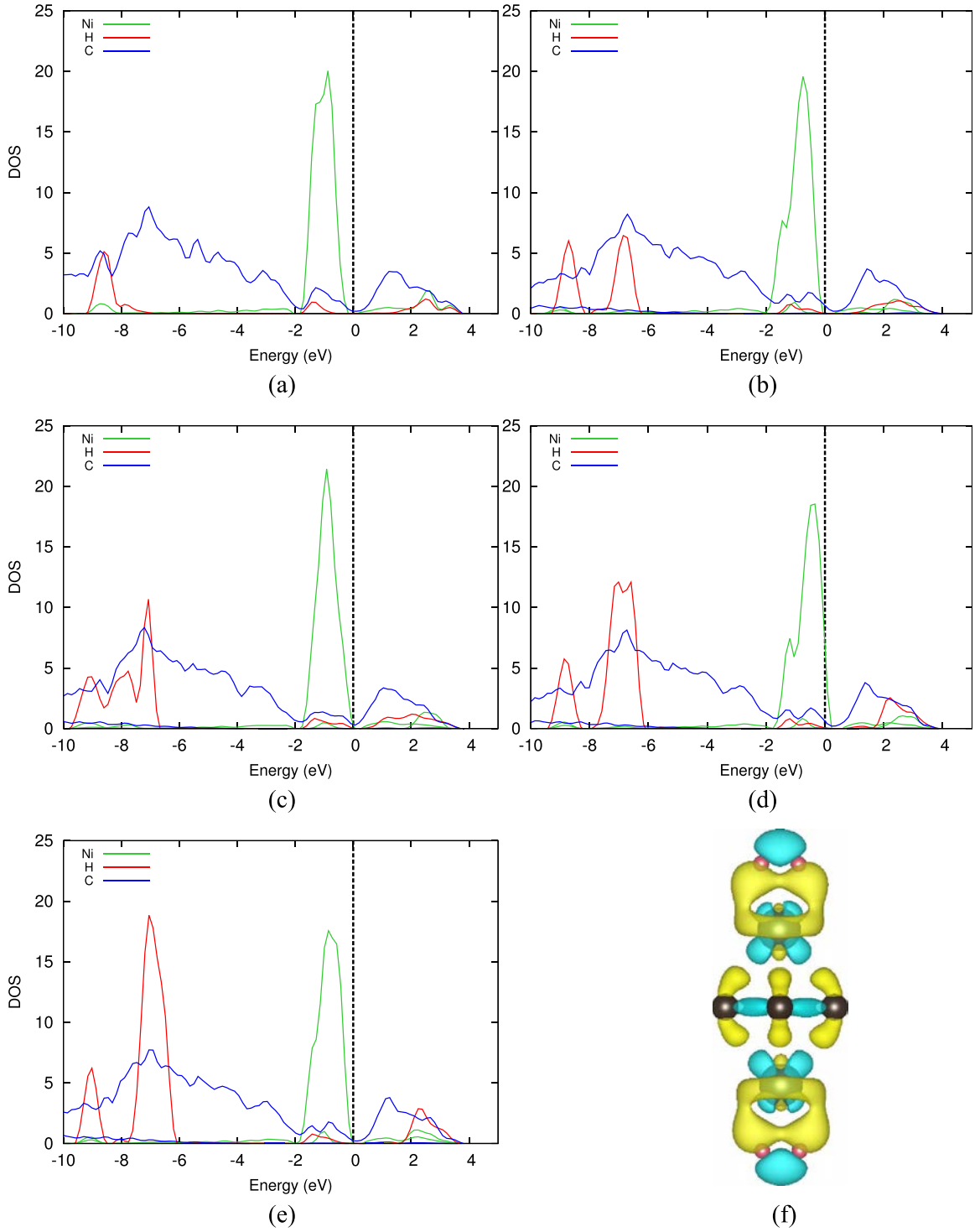

FIG. 11. PDOS of 16 carbon Ni decorated supercell system with increasing numbers of adsorbed hydrogen molecules: (a) 2, (b) 4, (c) 6, (d) 8, and (e) 10. The Fermi level is indicated by a dashed line. The charge density difference of the system with 2 hydrogen molecules (red colored atoms) adsorbed is shown in (f), where yellow indicates regions of charge gain and blue indicates regions of charge loss and carbon atoms are black colored.

gains of additional hydrogen adsorption as a greater number of heavier carbon atoms actually decreases the mass fraction of hydrogen.

D. Discussion

The disjointed set of previous studies cannot be used to confidently evaluate the comparative performance of metal-graphene systems. This is because these earlier studies used different types of pseudopotentials, exchange-correlation functionals, DFT simulation package implementations, metal coverages, and calculation parameters such as number of k-points, vacuum spacing, and energy cutoffs. This points to the motivation for and one of the advantages of this paper's investigations, where the simulation of a large number of metals using the same consistent conditions allows the

proper comparison of these systems. Our results on the whole show less spectacular performance for metal decorated systems with regards to hydrogen storage as opposed to some earlier studies which have claimed very high hydrogen binding energies and gravimetric densities which easily exceed the DOE target of 5.5% wt. The lack of consideration of vdW forces, the use of small vacuum spacings and the use of the LDA functional, which is known to overpredict binding energies, likely all lead to earlier studies overestimating the hydrogen binding ability of metal decorated systems. In fact, several of the metal systems which previously reported studies claim can exceed the DOE's target (such as Al and Li) have been found in our investigations to be unable to meet this goal. On the other hand, even our best case result for Ni barely manages to surpass the DOE target in its theoretical gravimetric density. This value will likely decrease in real life conditions as part of a larger contained system and may turn out to be below the target value. This suggests that metal decoration alone will be unlikely to meet the DOE gravimetric density targets, although it can get us there most of the way. This is also likely one of the reasons that experimental results are not able to replicate the spectacular values claimed by earlier studies. Therefore, additional methods for increasing hydrogen adsorption abilities of graphene will have to be explored together with metal decoration. These could include manipulating the curvature or interlayer distance of the graphene substrate as suggested by Tozzini *et al.*[6] or defect engineering some of the graphene substrate as suggest by Yadav *et al.*[29] The combination of both approaches would lead to a higher hydrogen storage capacity than either one by itself and metal decoration would continue to play an important role in significantly increasing the hydrogen binding ability of graphene systems.

IV. CONCLUSIONS

The atomic adsorption ability of eight metals on graphene, four light metals, and four transition metals was investigated using the PBE-GGA functional first and then with the addition of the vdW-DF2 functional. The use of vdW-DF2 generally led to stronger binding of the metal adatom for lighter metals and weaker binding for heavier metals in comparison to GGA only simulations. Both single and double-sided decorations were found to obey the same trends and double sided decoration did not decrease system stability. Therefore, all subsequent simulations were carried out using double-sided decoration. The hydrogen binding ability of these metals was then investigated through the adsorption of a single hydrogen molecule over each adatom. The light metals were found to weakly bind hydrogen, whereas the transition metals displayed an order of magnitude stronger binding. The transition metals produced hydrogen-metal complexes where the hydrogen molecule had dissociated into individual atoms over a metal atom. Similar to metal atom binding, it was found that hydrogen binding ability was increased with the use of vdW-DF2 for light metals but decreased for transition metals.

Three metals (Cu, Ni, Pd) demonstrated hydrogen binding energies close to the range of 0.2–0.6 eV considered useful for practical reversible hydrogen storage. Among these, Ni was selected as the best candidate for a metal-graphene hydrogen storage system due to its low mass and stability in practical systems. The effect of varying metal coverage on a graphene sheet was investigated for four different sized (6–72 carbon atoms) supercells. It was found that decreasing metal coverage by increasing the supercell size (thereby increasing the number of carbon atoms per Ni atom) generally improved the hydrogen binding ability of the metal. Next, the gravimetric density of the three smallest supercells was studied as additional hydrogen molecules were adsorbed onto the system. The 16 carbon supercells displayed the best balance of small supercell size and ability to bind several hydrogen molecules (up to 10), giving it the highest produced gravimetric density of 6.12 wt. %.

Our investigations show that vdW forces can have a significant impact on simulation results. Corrections to better represent such forces should be applied with functionals, such as vdW-DF2, particularly as vdW forces play an important role in hydrogen interactions and adsorption. The inclusion of vdW forces was also found to decrease the hydrogen binding ability of transition metals, which means that earlier studies which neglected such effects might have overestimated the usefulness of metal adatoms for hydrogen adsorption. This could be a reason for the inability of experimental studies to replicate the phenomenal hydrogen storage results of theoretical metal decoration studies. Our results suggest that even the best case scenario would produce a gravimetric density of 6.12 wt. %, just above the DOE target of 5.5 wt. %. This means that additional techniques for enhancing hydrogen storage, such as graphene sheet curvature and defect engineering, should be investigated to be used in conjunction with metal decoration to produce a truly feasible real world hydrogen storage system.

ACKNOWLEDGMENTS

Computations were performed on the HPC supercomputer at the SciNet HPC Consortium[30] and Rèseau Quèbècois de Calcul de Haute Performance Consortium. SciNet is funded by the Canada Foundation for Innovation under the auspices of Compute Canada; the Government of Ontario; Ontario Research Fund—Research Excellence; and the University of Toronto. Financial support was provided by Natural Sciences and Engineering Council of Canada and the University of Toronto. The authors gratefully acknowledge their support.

[1]M. Pagliaro, A. G. Konstandopoulos, R. Ciriminna, and G. Palmisano, "Solar hydrogen: fuel of the near future," Energy Environ. Sci. **3**, 279–287 (2010).
[2]Y. Sun, Q. Wu, and G. Shi, "Graphene based new energy materials," Energy Environ. Sci. **4**, 1113–1132 (2011).
[3]A. Zttel, "Materials for hydrogen storage," Mater. Today **6**(9), 24–33 (2003).
[4]Targets for Onboard Hydrogen Storage Systems for Light-Duty Vehicles, Technical report, U.S. Department of Energy Office of Energy Efficiency and Renewable Energy and The Freedom CAR and Fuel Partnership, 2009.

[5]L. Firlej, B. Kuchta, C. Wexler, and P. Pfeifer, "Boron substituted graphene: Energy landscape for hydrogen adsorption," Adsorption **15**, 312–317 (2009).
[6]V. Tozzini and V. Pellegrini, "Prospects for hydrogen storage in graphene," Phys. Chem. Chem. Phys. **15**, 80–89 (2013).
[7]V. Wang, H. Mizuseki, H. P. He, G. Chen, S. L. Zhang, and Y. Kawazoe, "Calcium-decorated graphene for hydrogen storage: A van der Waals density functional study," Comput. Mater. Sci. **55**, 180–185 (2012).
[8]W. Zhou, J. Zhou, J. Shen, C. Oujang, and S. Shi, "First-principles study of high-capacity hydrogen storage on graphene with Li atoms," J. Phys. Chem. Solids **73**, 245–251 (2012).
[9]Z. M. Ao and F. M. Peeters, "High-capacity hydrogen storage in Al-adsorbed graphene," Phys. Rev. B **81**(20), 205406 (2010).
[10]C. Ataca, E. Aktürk, and S. Ciraci, "Hydrogen storage of calcium atoms adsorbed on graphene: First-principles plane wave calculations," Phys. Rev. B **79**, 041406 (2009).
[11]C.-H. Chen, T.-Y. Chung, C.-C. Shen, M.-S. Yu, C.-S. Ts, G.-N. Shi, C.-C. Huang, M.-D. Ger, and W.-L. Lee, "Hydrogen storage performance in palladium-doped graphene/carbon composites," Int. J. Hydrogen Energy **38**(9), 3681–3688 (2013).
[12]W. G. Hong, B. H. Kim, S. M. Lee, H. Y. Yu, Y. J. Yun, Y. Jun, J. B. Lee, and H. J. Kim, "Agent-free synthesis of graphene oxide/transition metal oxide composites and its application for hydrogen storage," Int. J. Hydrogen Energy **37**(9), 7594–7599 (2012).
[13]C.-C. Huang, Y.-H. Li, Y.-W. Wang, and C.-H. Chen, "Hydrogen storage in cobalt-embedded ordered mesoporous carbon," Int. J. Hydrogen Energy **38**(10), 3994–4002 (2013).
[14]H. Zhou, X. Liu, J. Zhang, X. Yan, Y. Liu, and A. Yuan, "Enhanced room-temperature hydrogen storage capacity in pt-loaded graphene oxide/hkust-1 composites," Int. J. Hydrogen Energy **39**(5), 2160–2167 (2014).
[15]P. Giannozzi, S. Baroni, N. Bonini, M. Calandra, R. Car, C. Cavazzoni, D. Ceresoli, G. L. Chiarotti, M. Cococcioni, I. Dabo *et al*. "Quantum espresso: A modular and open-source software project for quantum simulations of materials," J. Phys.: Condens. Matter **21**, 395502 (2009).
[16]J. P. Perdew, K. Burke, and M. Ernzerhof, "Generalized gradient approximation made simple," Phys. Rev. Lett. **77**(18), 3865–3868 (1996).
[17]The following pseudopotentials were used Al.pbe-n-van.UPF, C.pbe-rrkjus.UPF, C.pbe-van_ak.UPF, C.pbe-van_bm.UPF, Ca.pbe-nsp-van.UPF, Cu.pbe-n-van_ak.UPF, H.pbe-rrkjus.UPF, H.pbe-van_ak.UPF, H.pbe-van_bm.UPF, Na.pbe-sp-van_ak.UPF, Ni.pbe-nd-rrkjus.UPF, Pd.pbe-rrkjus.UPF, Pt.pbe-n-van.UPF, and Ti.pbe-sp-van_ak.UPF. The pseudopotential that was used for C and H corresponded to the metal decoration pseudopotential type to maintain consistency.
[18]K. Lee, E. D. Murray, L. Kong, B. I. Lundqvist, and D. C. Langreth, "Higher-accuracy van der waals density functional," Phys. Rev. B **82**, 081101 (2010).
[19]M. Dion, H. Rydberg, E. Schroder, D. C. Langreth, and B. I. Lundqvist, "Van der waals density functional for general geometries," Phys. Rev. Lett. **92**(24), 246401 (2004).
[20]H. J. Monkhorst and J. D. Pack, "Special points for brillouin-zone integrations," Phys. Rev. B **13**(12), 5188–5192 (1976).
[21]M. Methfessel and A. T. Paxton, "High-precision sampling for brillouin-zone integration in metals," Phys. Rev. B **40**, 3616–3621 (1989).
[22]J. Dai, J. Yuan, and P. Giannozzi, "Gas adsorption on graphene doped with b, n, al, and s: A theoretical study," Appl. Phys. Lett. **95**(23), 232105 (2009).
[23]A. Sigal, M. I. Rojas, and E. P. M. Leiva, "Is hydrogen storage possible in metal-doped graphite 2d systems in conditions found on earth?," Phys. Rev. Lett. **107**, 158701 (2011).
[24]A. Sigal, M. I. Rojas, and E. P. M. Leiva, "Interferents for hydrogen storage on a graphene sheet decorated with nickel: A DFT study," Int. J. Hydrogen Energy **36**(5), 3537–3546 (2011).
[25]A. Kokalj, "Computer graphics and graphical user interfaces as tools in simulations of matter at the atomic scale," Comput. Mater. Sci. **28**(2), 155–168 (2003).
[26]K. Momma and F. Izumi, "VESTA3 for three-dimensional visualization of crystal, volumetric and morphology data," J. Appl. Crystallogr. **44**(6), 1272–1276 (2011).
[27]I. Lopez-Corral, E. German, A. Juan, M. A. Volpe, and G. P. Brizuela, "DFT study of hydrogen adsorption on palladium decorated graphene," J. Phys. Chem. **115**, 4315–4323 (2011).
[28]G. J. Kubas, "Metal–dihydrogen and σ-bond coordination: The consummate extension of the Dewar–Chatt–Duncanson model for metalolefin bonding," J. Organomet. Chem. **635**(1–2), 37–68 2001).
[29]S. Yadav, Z. Zhu, and C. V. Singh, "Defect engineering of graphene for effective hydrogen storage," Int. J. Hydrogen Energy **39**(10), 4981–4995 (2014).
[30]C. Loken, D. Gruner, L. Groer, R. Peltier, N. Bunn *et al*., SciNet: Lessons learned from building a power-efficient top-20 system and data centre," J. Phys.: Conf. Ser. **256**, 012026 (2010).